Long time series of outputs from a geodynamo model approaching Earth's core conditions

Julien Aubert

4DEarth_Swarm_Core ESA project deliverable D-C.1

1 General description

This document refers to publicly available output data from a geodynamo simulation that approaches closely to the physical conditions of Earth's core. In the model parameter space, this model is part of a series that defines a path connecting the conditions where classical dynamo models are found to those of the Earth's core. The theoretical definition of this path may be found in Aubert et al. (2017), and the model described here is located at 71% of this path (path parameter $\epsilon = 10^{-5}$). This model is fully described in Aubert & Gillet (2021). The outputs that are made available here consist in coefficients describing the poloidal magnetic field outside the core, the diffusive part of the poloidal magnetic field temporal rate-of-change (the secular variation), and the coefficients describing the velocity field at the core surface. The model operates with stress-free boundary conditions, which implies that Ekman boundary layers are not described and that the core surface directly corresponds to the free stream. Table 1 lists the key time scales and associated dimensionless numbers of this model together with those expected at Earth's core conditions.

From the dimensionless outputs of the numerical model, the values of the velocity and magnetic field coefficients presented in the available data are **already scaled to dimensional values**, in nanoteslas for the magnetic field, nanoteslas per year for the diffusive part of the secular variation, and kilometers per year for the velocity field. Here I mention some details for the re-scaling procedure that has been applied. Re-scaling can be done in a completely self-consistent manner only once the model conditions reach those of the Earth's core. The path theory serves to rescale these quantities in a way that rationalizes the gap that still exists between those two conditions (Aubert, 2018, 2020). For the time series presented here, the time basis is provided by the choice of the magnetic diffusivity η in table 1. From there and the value of the magnetic Reynolds number Rm immediately follow the determination of the core overturn time τ_U involving the root-mean-squared flow velocity U in the shell and the re-scaling of the velocity field. The value of the Lundquist

Quantity	Definition	71% of path model	Earth's core
Earth radius	a	6371.2 km	6371.2 km
core surface radius	r_o	3485 km	3485 km
outer core thickness	D	2260 km	2260 km
magnetic diffusivity	η	1.2 m^2/s	$\approx$ 1.2 m^2/s
magnetic diffusion time	$\tau_\eta = D^2/\eta$	135000 yr	$\approx$ 135000 yr
planetary rotation period	$2\pi\tau_\Omega = 2\pi/\Omega$	12 days	1 day
Alfvén time	$\tau_A = \sqrt{\rho\mu}D/B$	5.8 yr	$\approx$ 2 yr
1D Alfvén speed	$D/\sqrt{3}\tau_A$	225 km/yr	$\approx$ 650 km/yr
core overturn time	$\tau_U = D/U$	118 yr	$\approx$ 120 yr
1D convective speed	$D/\sqrt{3}\tau_U$	11 km/yr	$\approx$ 11 km/yr
Magnetic Ekman number	$E/Pm = \tau_\Omega/\tau_\eta$	$3.8\ 10^{-8}$	$\approx 3.2\ 10^{-9}$
Magnetic Reynolds number	$Rm = \tau_\eta/\tau_U$	1140	$\approx$ 1100
Lundquist number	$S = \tau_\eta/\tau_A$	23300	$\approx$ 68000

Table 1
Key parameters for the model, presented together with their model values and values expected at Earth's core conditions. B and U are root-mean-squared amplitudes of the magnetic field inside the simulated core.

number gives access to the Alfvén time τ_A, which however differs from its target Earth value as we are not yet at the end of the path. The r.m.s dimensional magnetic field amplitude B can therefore be obtained by considering that the density ρ of the simulated fluid shell is $(5.8/2)^2$ time stronger than its Earth counterpart $\rho = 11000\ kg/m^3$, this former factor accounting for the differences in the model and Earth Alfvén times.

Figure 1 presents temporal sequences of the core-mantle boundary secular acceleration energy (as defined in Aubert, 2018) and Earth-surface jerk energy (as defined in Aubert & Finlay, 2019). The sequence contained in the data files starts at timestamp 4200 years. The preceding temporal sequence is not proposed as it contains a number of changes in model resolution, output resolution, time step that have followed from the need to tackle numerical instabilities and from discussions within the consortium, which make this earlier part of the model unsuitable for public release. The duration of the released sequence is 10000 years. The numerical time step used for the computation is 0.3 hours. Outputs have been recorded at a sampling rate of 30 hours. The sampling rate selected for public release is 0.2 years. The consortium is free to discuss whether a faster delivery sampling rate is needed, but it should be kept in mind that this comes at the cost of file size. Furthermore, we have previously

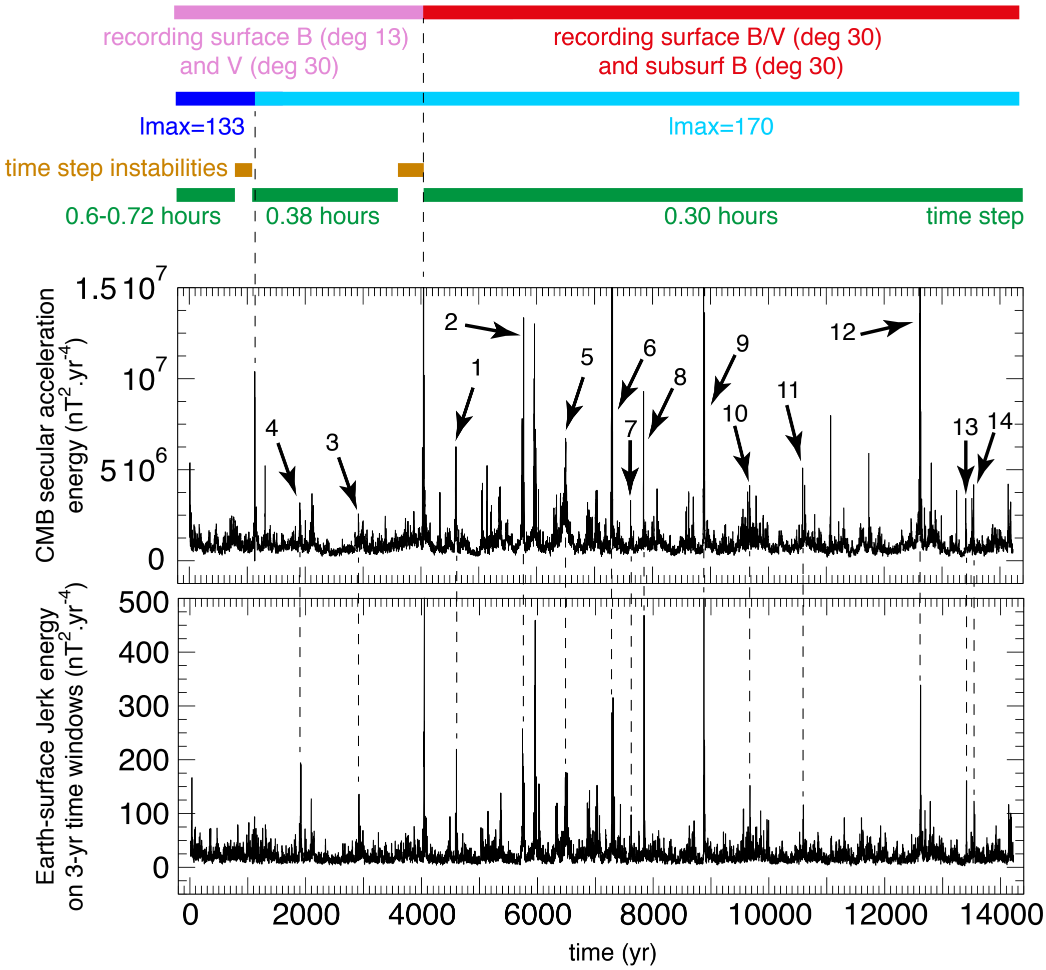

Fig. 1. Core-mantle boundary (CMB) secular acceleration energy (top) and Earth-surface jerk energy (bottom), as functions of the dimensional simulation time. See Aubert (2018); Aubert & Finlay (2019) for definitions. The outputs have been truncated here at spherical harmonic degree and order 13 (which is the minimum spatial resolution for outputs of the whole sequence), but the publicly available outputs are supplied up to a higher spherical harmonic resolution of 30. The colored bands above the graphs locate notable events in the simulation concerning the nature and maximum spherical harmonic degree of outputs (pink/red), the native spherical harmonic degree ℓ_{max} of the computation (blue/cyan), the computation time step values (green) and encountered instabilities thereof (brown).

shown (Aubert, 2018) that the signal contains almost no energy at periods shorter than the planetary rotation period $2\pi\tau_\Omega$ = 283 hours = 11.8 days = 0.03 years. The time stamps for notable jerk events are reported in table 2.

2 Data format and description

The file format is MATLAB `.mat`.

Jerk No.	timestamp (years)
1	4600
2	5750
5	6490
6	7300
7	7620
8	7840
9	8880
10	9673
11	10590
12	12620
13	13411
14	13546

Table 2
Approximate timestamps for notable jerks in the publicly available part of the sequence.

2.1 Magnetic field coefficients

To describe the magnetic field at and above the core surface, we adopt the classical Gauss coefficient description for the magnetic field. Denoting the colatitude as θ and the Greenwich-centered longitude as φ, the poloidal field at a radius r above the core-mantle boundary may be written

$$\mathbf{B}_{\boldsymbol{p}}(r, \theta, \varphi, t) = -\boldsymbol{\nabla} V \tag{1}$$

where

$$V(r, \theta, \varphi, t) = a \sum_{l=1}^{30} \left(\frac{a}{r}\right)^{l+1} \sum_{m=0}^{l} \left[g_l^m(t) \cos m\varphi + h_l^m(t) \sin m\varphi\right] P_l^m(\cos\theta). \tag{2}$$

Here t is time, $a = 6371.2$ km is Earth's magnetic radius of reference, P_l^m is the Schmidt-seminormalised Legendre function of degree l and order m.

The file `Gauss_Bsurf.mat` comprises the dimensional timestamp vector `timers` containing the discrete values of t and an array `gnm` containing the coefficients $g_l^m(t)$, $h_l^m(t)$ arranged according to:

$$
\begin{aligned}
\texttt{gnm}(:,1) &= g_1^0(t)\\
\texttt{gnm}(:,2) &= g_1^1(t)\\
\texttt{gnm}(:,3) &= h_1^1(t)\\
\texttt{gnm}(:,4) &= g_2^0(t)\\
\texttt{gnm}(:,5) &= g_2^1(t)\\
\texttt{gnm}(:,6) &= h_2^1(t)\\
\texttt{gnm}(:,7) &= g_2^2(t)\\
\texttt{gnm}(:,8) &= h_2^2(t)\\
&\dots\\
\texttt{gnm}(:,959) &= g_{30}^{30}(t)\\
\texttt{gnm}(:,960) &= h_{30}^{30}(t)
\end{aligned}
$$

Note that the sinus coefficients corresponding to $m = 0$ are not stored as they vanish identically. There are therefore 960 coefficients corresponding to a description of the output up to spherical harmonic degree and order 30. The core surface poloidal magnetic field is then obtained by setting r to $r_o = 3485$ km in equation (2).

In file `Gauss_Magdiff.mat` the Gauss coefficients corresponding to the diffusive part $\eta\nabla^2\mathbf{B}_p$ of the secular variation $\partial\mathbf{B}_p/\partial t$ below the core surface are encoded in the variable `dgnm` together with the time stamp `timers`. The advective part of the secular variation can then be obtained by taking the centered finite differences of variable `gnm` from file `Gauss_Bsurf.mat` and subtracting `dgnm` to the result. The magnetic diffusion obviously does only make sense at the core surface i.e. by setting r to $r_o = 3485$ km in equation (2), but its representation in terms of the same Gauss coefficients as those used for the poloidal field allows to quickly apprehend its contribution to the total secular variation, and also to quickly convert the output to a radial magnetic field, which is the representation that is usually preferred to cast the magnetic induction equation at the core surface.

2.2 Velocity field coefficients

The core surface velocity field coefficients are described using the spheroidal-toroidal formalism. The θ and φ components of the core surface velocity vector $\mathbf{u}$ are written

$$
\mathbf{u} = \begin{pmatrix} u_\theta = \dfrac{1}{\sin\theta}\dfrac{\partial T}{\partial\varphi} + \dfrac{\partial S}{\partial\theta} \\ u_\varphi = -\dfrac{\partial T}{\partial\theta} + \dfrac{1}{\sin\theta}\dfrac{\partial S}{\partial\varphi} \end{pmatrix} \tag{3}
$$

The spectral decomposition of T, S obeys

$$T = \sum_{l=1}^{30} \sum_{m=0}^{l} \left[tc_l^m(t) \cos m\varphi + ts_l^m(t) \sin m\varphi\right] P_l^m(\cos\theta) \tag{4}$$

$$S = \sum_{l=1}^{30} \sum_{m=0}^{l} \left[sc_l^m(t) \cos m\varphi + ss_l^m(t) \sin m\varphi\right] P_l^m(\cos\theta) \tag{5}$$

The file `Gauss_Vsurf.mat` contains the timestamp `timers` together with two arrays `tnm` and `snm` where the coefficients tc_l^m,ts_l^m and sc_l^m,ss_l^m are respectively stored. The ordering follows that of the magnetic field Gauss coefficients i.e.

$$\begin{aligned}
\texttt{tnm}(:,1) &= tc_1^0(t)\\
\texttt{tnm}(:,2) &= tc_1^1(t)\\
\texttt{tnm}(:,3) &= ts_1^1(t)\\
\texttt{tnm}(:,4) &= tc_2^0(t)\\
\texttt{tnm}(:,5) &= tc_2^1(t)\\
\texttt{tnm}(:,6) &= ts_2^1(t)\\
\texttt{tnm}(:,7) &= tc_2^2(t)\\
\texttt{tnm}(:,8) &= ts_2^2(t)\\
&\ldots\\
\texttt{tnm}(:,959) &= tc_{30}^{30}(t)\\
\texttt{tnm}(:,960) &= ts_{30}^{30}(t)
\end{aligned}$$

Note that the sinus coefficients corresponding to $m = 0$ are not stored as they vanish identically. As for the magnetic field coefficients above there are 960 coefficients for each scalar, corresponding to a description of the output up to spherical harmonic degree and order 30.

References

Aubert, J., 2018. Geomagnetic acceleration and rapid hydromagnetic wave dynamics in advanced numerical simulations of the geodynamo, *Geophys. J. Int.*, **214**(1), 531–547.

Aubert, J., 2020. Recent geomagnetic variations and the force balance in Earth's core, *Geophys. J. Int.*, doi: 10.1093/gji/ggaa007.

Aubert, J. & Finlay, C. C., 2019. Geomagnetic jerks and rapid hydromagnetic waves focusing at Earth's core surface, *Nature Geosci.*, **12**(5), 393–398.

Aubert, J. & Gillet, N., 2021. The interplay of fast waves and slow convection in geodynamo simulations nearing Earth's core conditions, *Geophys. J. Int.*, doi: 10.1093/gji/ggab054.

Aubert, J., Gastine, T., & Fournier, A., 2017. Spherical convective dynamos in the rapidly rotating asymptotic regime, *J. Fluid. Mech.*, **813**, 558–593.